SPECTROSCOPIC OBSERVATIONS OF 10 EMISSION-LINE DWARF GALAXIES

T. D. KINMAN
Kitt Peak National Observatory[1]

AND

K. DAVIDSON[2]
University of Minnesota, Minneapolis
Received 1980 May 29; accepted 1980 July 15

ABSTRACT

Oxygen, helium, and neon abundances are derived from image-dissector scanner observations of 10 emission-line dwarf galaxies. The $n(O)/n(H)$ ratios range from 0.025 to 0.5 the solar value, with the expected anticorrelation with gas temperature. Assuming that $n(Ne^{++})/n(O^{++}) \approx n(Ne)/n(O)$, we find a value of 0.23 for this ratio, which is about 50% higher than the values quoted for Orion and the Magellanic Clouds. The mean ratio of $n(He^+, He^{++})/n(H^+)$ is 0.082 ± 0.007 for the five best observed galaxies: we do not detect any correlation of this ratio with the oxygen abundance. Reasons are given to refrain from deriving nitrogen abundances for these galaxies. It seems likely that the underlying continua in these galaxies come predominantly from mixtures of O-type stars and moderately hot giants and supergiants.

Absolute photographic magnitudes, hydrogen masses, and total masses are derived from *UBV* photometry and 21 cm H I observations of these galaxies. The ratio of H I mass to total mass increases monotonically with decreasing total mass. However, the Virgo dwarfs A 1228 + 12 and IC 3453 appear to be abnormally deficient in H I for their total masses. The H I content of each may have been modified by its past environment. A decrease in the $n(O)/n(H)$ ratio with decreasing galaxy mass is confirmed, but the scatter is too large for the functional form of the relation to be defined precisely. The emission-line equivalent width of $H\beta$ decreases with distance for the galaxies in our sample; this effect is probably caused by observational selection.

Subject headings: galaxies: photometry — galaxies: structure — nebulae: abundances

I. INTRODUCTION

"Dwarf" galaxies of the Magellanic type tend to be irregular in appearance, presumably because star formation occurs sporadically both in space and in time. They also have lower surface brightnesses than giant galaxies. The idea of "flashing dwarf galaxies" came with the work of Sargent and Searle (1970) on what they called "extragalactic H II regions," which appear to be prominent emission nebulae in relatively inconspicuous dwarf galaxies. Perhaps "compact blue galaxies" are basically similar cases of the same phenomenon, i.e., low-surface-brightness dwarf galaxies which are undergoing bursts of star formation.

Dwarf galaxies are traditionally and rather arbitrarily defined in terms of optical intrinsic luminosity: $M_{pg} \geq -15$ according to Hodge (1971), although brighter limits are sometimes used. A definition in terms of mass would have more physical significance (though less operational convenience), if mass is the main parameter that determines the evolution of the galaxy. Thus, protogalaxies with masses greater or less than $10^{10} M_{\odot}$ tend to fragment into larger or smaller subunits which (through

supernovae) produce larger or smaller amounts of heavy elements, respectively (see Reddish 1978). More massive galaxies might also be more capable of retaining their gaseous components. A relation between mass and chemical composition is therefore to be expected. Some dwarf galaxies (e.g., I Zw 18; see Searle 1976) are indeed known to have abnormally low oxygen/hydrogen ratios, but quantitative generalization awaits a larger body of data than is presently available. Fisher and Tully (1975), in their H I survey of the DDO dwarf galaxies, found little variation in the ratio of total mass to optical luminosity over a range of 10 mag in absolute magnitude, while the ratio of H I mass to optical luminosity is significantly greater in the dwarfs. This implies that the fraction of total mass which has been turned from gas into stars is smaller in a dwarf than in a giant galaxy.

In establishing relationships which depend upon absolute magnitude, observations of the intrinsically faintest objects will be very important. Observations of faint dwarf galaxies beyond the Local Group are unfortunately difficult to interpret because of uncertainties in their distances. Photoelectric observations are needed not only for total fluxes but also to investigate the nature of the faint extended parts of these galaxies from their colors. We also need 21 cm observations, in order to obtain redshifts, H I masses, and total (dynamical) masses. A

---

program of photoelectric photometry of dwarf galaxies was started at Kitt Peak in 1977, while a series of 21 cm observations at Arecibo were made with E. K. Conklin in that year (Kinman 1978); a detailed description of that work is in preparation (Kinman and Conklin 1981). Ten of the galaxies have localized regions whose emission-line spectra are bright enough, relative to their continua, for reliable spectroscopic analysis. These form the subject of this paper.

Positional, photometric, and radio data for these galaxies are listed in Table 1, in columns as follows: (1), (2), and (3) Identifications with references. (4) Equatorial coordinates (1950). (5) Galactic coordinates. (6) $(B-V)$ and $(U-B)$ colors for the largest aperture Δ in which both have been measured. (7) Δ in arcsec. (8) Interstellar extinction in our Galaxy, computed from the formula given by Sandage (1974). (9) Photographic magnitude B_H within the Holmberg diameter a_H which is given in arcsec. (10) Galactocentric radial velocity V_0 in km s^{-1} and distance D in Mpc, derived from V_0 assuming $H = 55$ km s^{-1} Mpc^{-1}. (Exceptions: IC 3258 and IC 3453 were both assumed to belong to the Virgo cluster and to be at the same distance as A1228+12, which has the same velocity as M87). (11) Absolute photographic magnitude, applying only the correction for extinction in our own Galaxy. (12) Log photographic luminosity L in solar units. (13) Log neutral hydrogen mass M_H in solar units. (14) Full half-power width ΔV of 21 cm line profile in km s^{-1}, after correction for instrumental broadening. These data are taken from Kinman and Conklin (1981) unless otherwise noted.

If $H = 55$ km s^{-1} Mpc^{-1}, these galaxies seem to have absolute magnitudes $-14.5 \geq M_{pg} > -17.8$; if $H = 100$ km s^{-1} Mpc^{-1}, they are 1.3 mag fainter. However, corrections for tilt and internal reddening would make them brighter. In appearance, they range from objects like A1116+51, A1228+12, and A2228−00, which appear almost stellar in the telescope, to IC 3258, an extended irregular of moderate surface brightness studied by Demoulin and Burbidge (1969), and DDO 64, which has an extended low-surface-brightness disk with two localized H II regions (Braccesi et al. 1972). Whether IC 3258 and IC 3453 are members of the Virgo cluster or not is somewhat controversial; their distances and magnitudes are therefore uncertain. The nature of II Zw 40 is also uncertain; in the radio it has a diameter of 4′, but in a crowded low-latitude field with considerable interstellar extinction, its optical size is difficult to determine.

II. THE EMISSION-LINE SPECTRA

Table 2 summarizes a number of digital spectra obtained in 1977–1978, using the KPNO 2.1 m telescope and intensified image dissector scanner (IIDS). Each spectrum includes light within a 6″.1 diameter circular region. Our " blue " spectra covered the range 3300–5100 Å, while our " red " spectra covered 5000–6800 Å. These were sky-subtracted, calibrated, and reduced using standard KPNO routines, except that a minor program defect required corrections of the order of 20% to fluxes near the edges of the red wavelength band. After slight smoothing,

the spectral resolution was ∼8 Å, depending somewhat upon the distribution of emission within each 6″ circle.

The spectra of DDO 64 refer to the more compact and southerly of the two H II regions in this object discussed by Braccesi et al. (1972). The spectrum of IC 3453 refers to the bright H II region 15″ south of the galaxy's center. The spectrum of Markarian 450 refers to the prominent condensation 7″ northwest of the galaxy's center.

We cannot rely upon using absolute flux measurements to match the blue and red spectra together; even small pointing and guiding errors and seeing variations will change the observed fluxes. Because we are primarily interested in *relative* line intensities, which should have less positional dependence than the absolute intensities, we have connected the red with the blue spectra by referring to the [O III] $\lambda5007$ line, which is measurable in both. Thus, the Hβ fluxes listed for red spectra in Table 2 are actually obtained by multiplying the red spectra $\lambda5007$ fluxes by the corresponding blue spectra H$\beta/\lambda5007$ intensity ratios. For Mrk 600, II Zw 40, DDO 64, and A2228−00, our "red" and "blue" Hβ flux estimates agree within 15%; but there are notable discrepancies for I Zw 18 (a factor of 1.8) and A1228+12 (a factor of 1.6), even though our spectra of these two objects have quite good signal-to-noise ratios. Small pointing errors are probably responsible for these discrepancies; there is no reason to doubt the reliability of line ratios in each spectrum.

Table 3 shows the relative line intensities, after reasonable corrections for interstellar reddening, if $\lambda5007$ is used as the red-blue link in each case. Our only useful reddening indicator is the Balmer decrement; we have estimated reddening corrections E_{B-V} (listed in Table 3) from the apparent Hα/Hβ/Hγ intensity ratios, assuming that these are purely recombination lines. Several difficulties occur with such estimates: (1) Hα was measured in red spectra while Hβ and Hγ were measured in blue spectra. Thus, for reasons mentioned above, and consistent with our treatment of other red spectrum lines in Table 3, we have assumed in each case (apparent Hα/Hβ ratio) = (H$\alpha/\lambda5007$ ratio in red spectrum × $\lambda5007$/Hβ ratio in blue spectrum). (2) Some of the H II temperatures mentioned below are so high that the Hα emission might be partly due to collisional excitation of hydrogen atoms rather than to recombination. This depends upon the equilibrium fraction of un-ionized hydrogen in each H II region, which depends upon the radiation/gas density ratio. Probably this effect is not very important. (3) The underlying stellar continua probably have Balmer absorption lines, which would reduce the apparent Balmer emission intensities, especially beyond Hβ. The most likely source of the continua (see § III) are early type stars whose spectra may have equivalent widths of the order of 3 or 4 Å for the Hβ and Hγ absorption lines; these are considerably smaller than the observed emission equivalent widths, except in the case of IC 3453 (see Table 2), so this difficulty is probably not very serious. (The objects discussed here were particularly chosen to have large emission line/continuum intensity ratios.) Our adopted extinction law as a function of wavelength was

TABLE 1
PHOTOMETRIC, RADIO, AND POSITIONAL DATA

Object (1)	Alternate Name (2)	Ref. (3)	α,δ (1950) (4)	ℓ,b (deg) (5)	$(B-V)$ $(U-B)$ (6)	Δ (arcsec) (7)	A_B (mag) (8)	B_H a_H (9)	V_0 D (10)	M_{pg} (11)	log L (12)	log M_H (13)	ΔV (14)
Mkn 600	MCG 1-08-008	a,b	02^h48^m5 $+04°15'$	170 -47	0.44 -0.26	12	0.04	15.42 51"	+1027 18.7	-15.98	8.58	8.56	72
II Zw 40	N A0116	c,d	05^h53^m1 $+03°23'$	203 -10	0.89 0.20	12	1.26	15.60 64"	+689 12.5	-16.14	8.65	8.80[p]	—
I Zw 18	N A0166 Mkn 116 Zw 0930+55	d,e,f	09^h30^m5 $+55°28'$	161 45	0.09 -0.61	24	0.06	16.17 36"	+802 14.6	-14.48	7.98	8.2:[q]	—
DDO 64	UGC 5272 MCG 5-23-041	b,g,h	09^h47^m4 $+31°43'$	195 51	0.33 -0.44	24	0.00	(14.5) 156"	+463 8.4	-15.12	8.24	8.48	77
A1116+51	Arp dwarf	i,j	11^h16^m7 $+51°46'$	152 60	0.10 -0.66	19	0.00	17.07 16"	+1420 25.8	-14.99	8.19	8.42[r]	80[r]
IC 3258	UGC 7470 MCG 2-32-021	b,h,k	12^h21^m2 $+12°45'$	278 74	0.34 -0.39	48	0.00	13.84 100"	-500 21.2	-17.79	9.31	8.42	100:
A1228+12	RMB 132	i,ℓ	12^h28^m3 $+12°19'$	284 74	0.11 -0.48	11	0.00	17.06 23"	+1165 21.2	-14.57	8.02	7.83	95
IC 3453	UGC 7666 MCG 3-32-057 RMB 25	b,h,k	12^h29^m1 $+15°08'$	281 77	0.47 -0.53	85	0.00	14.78 78"	+2473 21.2	-16.50	8.79	8.15	95
Mkn 450	UGC 8323 MCG 6-29-065	b,h,m	13^h12^m5 $+35°09'$	92 81	0.52[o] -0.44[o]	56	0.00	14.50 88"	+915 16.6	-16.60	8.83	8.40	66
A2228-00	Kinman dwarf HL 293B	i,n	22^h28^m0 $-00°23'$	66 -47	0.29 -0.34	6	0.04	17.72 17"	+1768 32.1	-14.85	8.13	8.27	60:

REFERENCES.—(a) Markarian 1973. (b) Vorontsov-Veljaminov 1962-68. (c) Sargent 1970. (d) Nilson 1974. (e) Zwicky 1966. (f) Markarian 1969. (g) van den Bergh 1959. (h) Nilson 1973. (i) de Vaucouleurs, de Vaucouleurs, and Corwin 1976. (j) Dreyer 1910. (k) Arp 1965. (l) Rubin, Moore, and Bertiau 1967. (m) Markarian 1972. (n) Kinman 1965. (o) Huchra 1977. (p) Gottesman and Weliachew 1972. (q) Chamaraux 1977. (r) Kinman et al. 1977.

TABLE 2

JOURNAL OF SPECTROSCOPIC OBSERVATIONS

Object	Date (UT)		t (min)	Wave-band[a]	F(Hβ)[b]	W(Hβ)[c]
Mkn 600.....	1977 Dec. 13		20	blue	2.7	50
	1977 Dec. 15		10	red	2.4	——
II Zw 40....	1977 Dec. 14		40	blue	9.0	250
	1977 Dec. 15		30	red	8.7	——
I Zw 18.....	1977 Dec. 13		60	blue	2.0	97
	1977 Dec. 15		40	red	3.6	——
DDO 64[d].....	1977 Dec. 13	15⎫		blue	1.9	180
	1977 Dec. 14	40⎬				
	1977 Dec. 15	20		red	1.7	——
A1116+51....	1978 Jan. 1		10	blue	1.2	40:
IC 3258.....	1977 Feb. 15		15	blue	4.6	130
A1228+12....	1977 Feb. 14		10	blue	2.1	86
	1977 Dec. 13		60	blue	2.4	83
	1977 Dec. 15		40	red	1.5	——
IC 3453[e]....	1977 Feb. 15		15	blue	1.1	25
Mkn 450[f]....	1978 Jan. 13		14	blue	7.1	270:
A2228-00....	1977 Dec. 14		60	blue	1.06	92
	1977 Dec. 15		20	red	1.13	——

[a]Blue is λλ3300–5100 Å, and red is λλ5000–6800 Å.

[b]Hβ flux (in units of 10^{-14} erg cm^{-2} s^{-1}) refers to 6".1 diameter regions as seen from above the Earth's atmosphere; no corrections for galactic extinction have been made. F(Hβ) for red wavebands are indirect values equal to the product of the [O III] 5007 flux and the Hβ/[O III] 5007 ratio measured in the blue waveband.

[c]"Equivalent width" of Hβ in Å.

[d]Southwest of two H II regions described by Bracessi et al. (1972).

[e]H II region ~15" south of galaxy center.

[f]H II region ~7" northwest of galaxy center.

quite conventional, essentially that used by Lequeux et al. (1979). In determining E_{B-V}, the Hα, Hβ, and Hγ lines were given (rather arbitrarily) relative weights of 2, 4, and 3 respectively; then the derived values of E_{B-V} were rounded to the nearest tenth (except for Mrk 600 and II Zw 40).

Subjective and perhaps rather pessimistic uncertainties in the measurements are indicated in Table 3 by letters a, b, c, and d which correspond roughly to ±10%, ±15%, ±25% and >25%, respectively; these involve the signal-to-noise ratios but do not take systematic errors, e.g., due to reddening corrections or to the red/blue matching, into account. The listed Hα/Hβ/Hγ/Hδ and He I λ4471/λ5876 intensity ratios are satisfyingly in accord with theoretical values for these recombination lines. Lequeux et al. (1979) have described independent observations of I Zw 18 and II Zw 40, made with the same equipment, and our data agree with theirs quite well. For I Zw 18, rms fractional discrepancy between their values and ours is less than

15%. (The worst discrepancy is for He I λ4471, which Lequeux et al. have marked as uncertain.) For II Zw 40, the rms discrepancy for Hγ and fainter lines is 10%; and for brighter lines, excepting [O II] λ3727, it is 5%. However, our λ3727 intensity is 30% less than theirs. The old λ3727 measurement by Sargent and Searle (1970) agrees with Lequeux et al. and not with us. This feature is intense enough to measure well, and different reddening cannot explain the discrepancy. Being a relatively low-excitation feature, [O II] λ3727 may be relatively more intense at the outer edges of the condensation in II Zw 40; and since Lequeux et al. used a 3".8 × 12".4 aperture, their observations refer to a slightly different region, which may explain the discrepancy. (Sargent and Searle do not specify their aperture.) The [N II] λ6584 line may be relevant to this point. In the spectrum of II Zw 40, we measured several faint lines not included in Table 3; one of them is λ6584, which we found to have about 0.021 as much intensity as

TABLE 3
RELATIVE LINE INTENSITIES

Line	Mkn 600	II Zw 40	I Zw 18	DDO 64	A1116+51	IC 3258	A1228+12	IC 3453	Mkn 450	A2228−00
3726, 3729 [O II]	167.0 a	80.0 a	33.0 b	136.0 a	200.0 ab	290.0 a	127.0 a	250.0 b	240.0 a	82.0 a
3835 Hη	—	8.0 b	—	—	—	—	—	—	7.0 b	—
3869 [Ne III]	72.0 a	61.0 a	21.0 b	38.0 a	43.0 b	18.0 b	42.0 a	37.0 b	49.0 a	51.0 a
3889 Hζ, He I	25.0 c	20.0 b	17.0 b	19.0 ab	24.0 b	1.5 b	19.0 b	—	23.0 b	17.0 b
3968 He I, [Ne III]	31.0 bc	34.0 a	18.0 b	—	—	19.0 b	26.0 a	—	31.0 a	25.0 b
4102 Hδ	20.0 bc	25.0 a	23.0 ab	22.0 ab	24.0 b	23.0 b	24.0 a	—	27.0 a	21.0 b
4340 Hγ	50.0 ab	50.0 a	49.0 a	51.0 a	47.0 ab	47.0 a	52.0 a	44.0 a	46.0 a	47.0 a
4363 [O III]	15.0 c	10.0 ab	6.1 b	8.0 b	6.0 c	1.6 c	14.0 b	4.5 d	5.1 b	19.0 b
4471 He I	4.0 cd	4.4 b	3.1 c	3.5 bc	—	4.0 bc	4.7 c	6.5 d	3.2 b	6.0 cd
4686 He II	≤5.0	≤3.0	3.0 c	≤2.0	—	≤4.0	4.3 c	≤10.0	≤1.5	≤8.0
4861 Hβ	100.0 a	100.0 a	100.0 a	100.0 a	100.0 a	100.0 a	100.0 a	100.0 a	100.0 a	100.0 a
4959 [O III]	210.0 a	253.0 a	66.0 a	150.0 a	81.0 a	100.0 a	168.0 a	125.0 a	170.0 a	200.0 a
5007 [O III]	660.0 a	807.0 a	204.0 a	490.0 a	262.0 a	320.0 a	515.0 a	420.0 a	520.0 a	620.0 a
5876 He I	13.0 bc	7.3 b	7.3 bc	11.0 c	e	e	10.0 c	e	e	19.0 cd
6563 Hα	285.0 b	289.0 a	272.0 a	284.0 a	e	e	285.0 a	e	e	270.0 a
6717 [S II]	5.0 cd	5.4 b	—	6.0 c	e	e	13.0 c	e	e	} 14.0 c
6731 [S II]	3.0 cd	4.1 b	—	5.0 c	e	e	9.0 c	e	e	
E_{B-V}	0.45	0.88	0.20	0.00	0.50	0.00	0.10	0.00	0.30	0.30

Note.—Line intensities are relative to Hβ(100) and corrected for the interstellar reddening specified. The quality of the measurement (a, b, c, and d) is defined in the text. An unobserved waveband is shown by e.

Hα, i.e., intensity 6 on the scale used in Table 3. Lequeux *et al.* found $\lambda6584$ to have about 0.026 as much intensity as Hα; so the [N II] discrepancy, although not very significant (because of the faintness of the line, and its proximity to Hα), is comparable to and in the same direction as the [O II] discrepancy. The [O II] and [N II] quite plausibly may have emission space distributions which differ from those of the higher-excitation lines, so that different sized apertures and/or pointing differences can account for the discrepancy in II Zw 40. Fortunately, this discrepancy will not seriously affect our conclusions.

Temperatures and abundances can be derived from the data in Table 3. Making the approximation that each ionized region has uniform temperature, we have estimated temperatures from the [O III] $\lambda4363/\lambda4959$ ratios (Seaton 1975). Our neglect of possible temperature variations in each region will result in underestimates of the oxygen and neon abundances (cf. Peimbert and Torres-Peimbert 1977), but this effect should be slight because the temperatures are rather high. Note that we have used the $\lambda4959$ but not the $\lambda5007$ intensities— because our measured $\lambda4959/\lambda5007$ ratios tend to be about 0.32 rather than the expected 0.34, and we suspect this systematic effect to be related to the great brightness of the $\lambda5007$ line, or perhaps its proximity to the redward end of each blue spectrum.

Table 4 shows estimated temperatures and abundances. The abundance of each ion X is specified by number, relative to hydrogen, in the form $[12 + \log_{10} n(X)/n(H^+)]$. Estimated errors are partly subjective; we hope that the actual " standard errors "would be smaller than the quoted values. Some of the temperatures are quite high, and there is an obvious anticorrelation between temperatures and oxygen abundances—as expected for photoionized regions where oxygen is a major coolant. Some representative temperatures and abundances found in the Orion Nebula and in the Magellanic Clouds, according to Peimbert and Torres-Peimbert (1974, 1977) and Pagel *et al.* (1978), are also listed in Table 4.

Most of the helium abundances in Table 4 are unremarkable; if Mrk 600, I Zw 18, DDO 64, A 1228 + 12, and Mrk 450 are considered to give independent measures of some " standard helium abundance," then we find $n(He^+, He^{++})/n(H^+) = 0.082 \pm 0.007$ for this standard value. This is not perceptibly affected if the He II $\lambda4686$ emission in I Zw 18 and A 1228 + 12 arise in the envelopes of hot stars as suggested by Bergeron (1977). Only a small fraction of He^0 is likely to coexist with the H^+, judging from the weakness of [N II] emission (possible exceptions are IC 3258, IC 3453, and Mrk 450, whose temperatures are low and whose red spectra we did not obtain).

The high helium abundance estimated for A 2228 − 00 may be significant; both the $\lambda4471/H\beta$ and the $\lambda5876/H\alpha$ ratios, while uncertain, indicate large values $n(He^+)/n(H^+) \gtrsim 0.12$.

II Zw 40 again presents a discrepancy: The estimated $\lambda5876/\lambda4471$ intensity ratio, which should be 2.7, is only 1.7. Lequeux *et al.* (1979) estimate 2.0 for the same ratio in this object. If much of the continuum comes from very hot

(O type) stars, then conceivably the observed nebular He I lines may be contaminated by stellar He I absorption and/or emission.

The $(O^+ + O^{++})$ abundances, as listed in Table 4 and derived using emission coefficients given by Seaton (1975) and Pradhan (1976), should be close to the total oxygen abundances. The weakness of He II $\lambda4686$ recombination emission shows that very little of the helium is doubly ionized, which means that oxygen ions beyond O^{++} are scarce. Absence of significant [O I] $\lambda6300$ emission, along with other arguments, suggests that atomic oxygen is also negligible in the H II regions; most of the oxygen coexisting with H^+ is therefore O^+ and O^{++}. Our results for oxygen in I Zw 18 and II Zw 40 are in satisfactory agreement with those found by Lequeux *et al.* (1979).

The oxygen abundances listed in Table 4 span a remarkable range. In IC 3258 (which seems to be a rather different object from the others), the oxygen abundance is similar to that in the Large Magellanic Cloud, a factor of 2 or 3 below the Sun or the Orion Nebula. II Zw 40, IC 3453, and Mrk 450 have oxygen abundances intermediate between those in the Large and the Small Magellanic Clouds. Mrk 600 and DDO 64 have oxygen abundances like the SMC, while those of A1116 + 51, A1228 + 12, and A2228 − 00 are below the SMC by factors close to 2, i.e., only $\frac{1}{20}$ solar value. Finally, of course, I Zw 18 is famous because it has even less oxygen, by a further factor of 3. Gas temperatures and oxygen abundances are anticorrelated in the expected way, as shown in Figure 1.

Most of the relevant neon is probably Ne^{++}, so it is plausible to suppose that

$$n(Ne)/n(O) \approx n(Ne^{++})/n(O^{++}).$$

With this assumption, nine of the objects in Table 4 give an average $n(Ne)/n(O) = 0.23$ with an rms deviation of 0.035. (We have used neon emissivities given by Pradhan 1974.) But in A1116 + 51, $n(Ne^{++})/n(O^{++}) \approx 0.45$; our data on this object are not of high quality, and perhaps
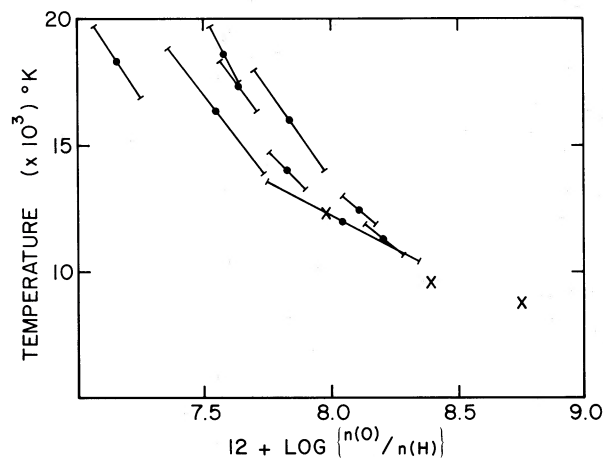

FIG. 1.—The anticorrelation of the gas temperature (*ordinate*) and the oxygen abundance (*abscissa*). The filled circles are the program galaxies, and the crosses are the SMC, LMC, and Orion.

TABLE 4

DERIVED TEMPERATURES AND ABUNDANCES

Object	T(°K)	Helium			Oxygen			Neon
		He⁺	He⁺⁺	He⁺,He⁺⁺	O⁺	O⁺⁺	O⁺,O⁺⁺	Ne⁺⁺
Mkn 600.......	16,000±2000	10.98±0.08	(≤9.7)	10.99±0.09	7.12±0.20	7.75±0.15	7.84±0.15	7.19±0.20
II Zw 40......	12,400± 500	10.87±0.2:	(≤9.4)	10.88±0.2:	7.11±0.10	8.08±0.05	8.12±0.06	7.44±0.07
I Zw 18.......	18,300±1500	10.82±0.08	9.43±0.15	10.84±0.08	6.23±0.13	7.11±0.07	7.16±0.09	6.49±0.12
DDO 64........	14,000± 800	10.91±0.08	(≤9.3)	10.92±0.09	7.17±0.08	7.72±0.08	7.83±0.08	7.07±0.08
A1116+51......	16,300±2400	10.91±0.10			7.18±0.20	7.30±0.20	7.55±0.20	6.95±0.25
IC 3258.......	9,300±1000	10.91±0.10	(≤9.5)	10.92±0.11	8.19±0.25	8.08±0.20	8.44±0.25	7.40±0.25
A1228+12......	17,300±1200	10.96±0.08	9.57±0.15	10.98±0.08	6.87±0.08	7.56±0.06	7.64±0.07	6.86±0.08
IC 3453.......	12,000±1600	11.13±0.15	(≤9.9)	11.14±0.16	7.66±0.45	7.83±0.30	8.05±0.35	7.28±0.45
Mkn 450.......	11,300± 600	10.82±0.08	(≤9.1)	10.82±0.09	7.74±0.09	8.03±0.07	8.21±0.08	7.48±0.09
A2228-00......	18,600±1300	11.18±0.08	(≤9.9)	11.19±0.09	6.61±0.07	7.58±0.06	7.62±0.06	6.87±0.07
Orion.........	(8700) av			11.00			(8.75) av	
LMC...........	(9600) av			10.91			(8.39) av	
SMC...........	(12,300) av						(7.98) av	

Note.—For each ion X, the abundance is specified in the form $\left[12 + \mathrm{Log}_{10} \dfrac{n(X)}{n(H^+)} \right]$.

there is an error involving reddening. In any case, regarding the other nine objects, $n(Ne)/n(O) \approx 0.23$ is about 50% higher than the values for Orion and the Magellanic Clouds quoted by Peimbert and Torres-Peimbert (1977), Pagel et al. (1978), and Lequeux et al. (1979). For II Zw 40 and I Zw 18, the Lequeux et al. Ne/O ratios are close to ours. Either these objects are modestly overabundant in neon relative to oxygen, or else, perhaps, temperature gradients in the emission regions are large enough to affect the [Ne III]/[O III] intensity ratios.

Nitrogen/oxygen ratios, while of great interest, cannot safely be estimated for objects like those discussed here. The emission regions are of rather high excitation so that most of the nitrogen is N^{++} rather than N^+, and this is awkward in two different ways. First, since N^+ is scarce, the [N II] emission is weak and difficult to measure (or even to detect, in most cases). We were able to estimate the [N II] $\lambda 6584$ intensity only for II Zw 40 and for DDO 64, obtaining values of about 6 (bc) and 7 (cd), respectively, on the intensity scale of Table 3. The second, and worse, difficulty is that the ionization fraction $n(N^+)/n(N)$ cannot be estimated reliably if $n(N^+) \ll n(N^{++})$, without knowing about the ionizing spectrum and geometrical situation in some detail. In general, the assumption that $n(N^+)/n(N^{++}) \approx n(O^+)/n(O^{++})$ is not justified, and for photoionization by stars with $T_{eff} > 40,000$ K, $n(N^+)/n(N^{++}) < n(O^+)/n(O^{++})$ is to be expected. The optical thickness of each ionized region is important, too, because O^+ and N^+ ions are concentrated (and perhaps concentrated differently) toward the low-excitation edge of a nebula. The size of the entrance aperture therefore affects the strength of the [N II] line which is measured. Moreover, temperature gradients are very likely to be important; note that the temperature dependence of [N II] $\lambda 6584$ differs from that of [O II] $\lambda 3727$. Recent notice of the importance of charge exchange (e.g., see Péquignot, Aldrovandi, and Stasinska 1978) should warn us that the concentrations of minority constituents in an ionization equilibrium cannot easily be calculated correctly. As a cautionary example, note the condensations in the Crab Nebula. These probably have rather similar N/O abundance ratios, and their [O II]/[O III] intensity ratios span only a moderate range of values (a factor of 2 or 3 variation), yet their [N II]/[O II] ratios vary greatly (a factor of 10 or so; see Davidson 1978, 1979; Miller 1978). In summary, there are good reasons to refrain from estimating nitrogen/oxygen abundance ratios in the high-excitation nebulae discussed here. Calculated photoionization models may be useful; but to give trustworthy results, these must employ realistic geometrical treatments more sophisticated than those in the literature. Similar statements can be made about the [S II] emission (Pagel 1978).

Finally, regarding line intensities, the [S II] $\lambda 6717/\lambda 6731$ ratio is somewhat greater than unity for some of the objects in Table 3. Using parameters given by Pradhan (1978), we deduce that the relevant electron densities are considerably below 1000 cm^{-3}, probably below 500 cm^{-3}; but the data are not good enough to justify more precise estimates.

The spectra of these galaxies (those with the highest temperatures) are sufficiently alike that we may reasonably combine them into a single spectrum. Figure 2 shows such a composite spectrum; the apparent spectra of Mrk 600, I Zw 18, DDO 64, A1228+12, and A2228−00 were shifted to zero velocity before adding them together. The strongest lines are truncated in the figure. We can see some weak features in the composite spectrum which are difficult to distinguish from noise in each individual spectrum. In particular, we see He II $\lambda 4686$, which may have a stellar origin. One must remember that these objects are larger and probably more
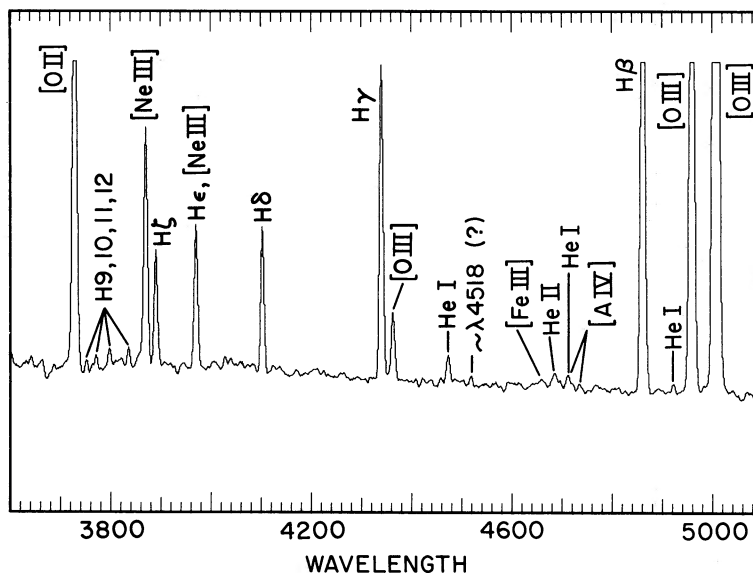

FIG. 2.—Composite spectrum obtained by adding the spectra of Mrk 600, I Zw 18, DDO 64, A1228+12, and A2228−00 after adjustment to zero velocity. The strongest lines ([O II] $\lambda 3727$, Hβ, and [O III] $\lambda\lambda 4959$, 5007) are truncated in this plot.

complicated than a typical Galactic emission nebula. They are regions of intense activity, and there may be components in the emission-line spectra from collisionally heated sources such as supernova remnants. In principle, the presence of supernova remnants might be inferred from nonthermal radio emission, but this would be difficult unless the sources are quite strong.

III. THE UNDERLYING CONTINUA

Next, we discuss the continuous spectra, remembering that the continua in our observations include just the 6″ diameter regions and not the entire galaxies. In order to relate the continua to the Hβ line intensities, and to avoid confusions of units, we shall discuss "dimensionless" continua,

$$Q_v = v_{H\beta} f_v / F_{H\beta} ,$$

where $v_{H\beta}$ is the frequency of Hβ, $F_{H\beta}$ is the energy flux in the Hβ line, and f_v is the continuum energy flux per unit frequency from the same region. Unless otherwise specified, Q_v includes a correction for reddening (E_{B-V} given in Table 3). The wavelength-equivalent width of Hβ in emission is simply

$$W_{H\beta} = \frac{4861 \text{ Å}}{Q_v(4861 \text{ Å})} .$$

The observed, de-reddened continua Q_v for most of our objects are shown in Figure 3. Here, continuous lines represent the "blue" data, dashed lines the "red" data; as with the emission lines, the [O III] λ5007 line has been used to relate the red spectra to Hβ. In the cases of I Zw 18, A1228 + 12, and A2228 − 00, there are obvious mismatches near 5000 Å, presumably due to pointing, guiding, and seeing differences between our blue and red observations. The "bump" in Q_v for IC 3453 may be erroneous, because of the relatively poor quality of the

data for this object. Figure 3 shows that the continua are "blue" by astronomical standards (note that Q_v = constant would have intrinsic colors $B - V = +0.10$ and $U - B = -0.90$; Matthews and Sandage 1963). However, most of these continua are not as blue as the Rayleigh-Jeans law, $Q_v \sim \lambda^{-2}$, which would occur if most of the 4000–6000 Å light came from stars hotter than 25,000 K. (*Exception:* the violet continuum of II Zw 40 resembles a Rayleigh-Jeans law, if no serious error has been made in the large and imprecise correction for reddening.)

The Balmer discontinuities are surprisingly weak, even after corrections have been made for the nebular Balmer continua. At the temperatures of interest, the nebular Balmer discontinuity in emission is about $\Delta Q_v \approx 10$. Appropriately corrected continua are shown by short dotted lines in Figure 3. It appears that the nebular and stellar Balmer discontinuities nearly cancel each other in several cases, e.g., II Zw 40. Note, however, that the measured continua are very uncertain between 3645 and 4000 Å (log λ = 3.56–3.60), because there are so many emission lines in this range; so the apparent smoothness of the continuous curves in Figure 3 may be partly illusory. After corrections, the absorption Balmer discontinuity is close to $\Delta \log Q_v = 0.15$ for Mrk 600, II Zw 40, DDO 64, IC 3258, and A2228 − 00, and about half as large for I Zw 18 and A1228 + 12. This suggests that most of the continuum light does not come from ordinary A or late B stars: their Balmer discontinuities would be too large. Cooler stars are unlikely too, because of the blue colors. Mixtures of ordinary O stars and moderately hot giants and supergiants are indicated; supergiants can have relatively small Balmer discontinuities. In order to produce He$^+$, O^{++} nebulae (i.e., with little [N II] emission), the stars that produce most of the ionizing radiation must be hotter than 35,000 K. (The number of helium-ionizing photons, $\lambda < 504$ Å, must exceed 0.1 times the number of
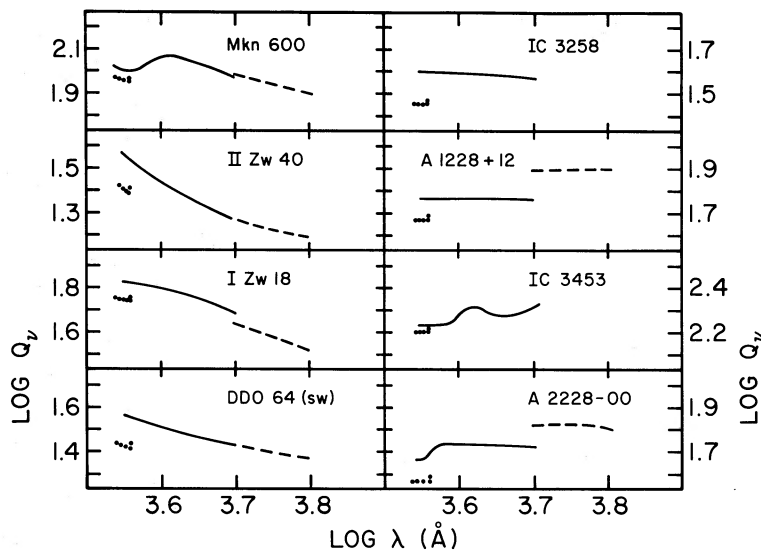

FIG. 3.—De-reddened continua (Q_v) as a function of wavelength: continuous lines represent "blue" data; dashed lines, the "red" data. Continua after correction for the nebula Balmer continua are shown by short dotted lines.

hydrogen-ionizing photons, $\lambda < 912$ Å; the factor 0.1 is roughly the helium abundance. See Auer and Mihalas 1972 for theoretical ionizing continua.) This seems consistent with remarks made by Bergeron (1977) and O'Connell, Thuan, and Goldstein (1978), but we note again that most of the observed continua are *not* as blue (in the $B - V$ sense) as O stars, unless there is additional reddening.

IV. REMARKS ABOUT THE REDDENING CORRECTIONS

In our reductions, we applied wavelength-dependent reddening corrections designed to correct each observed Balmer decrement to its theoretical, pure-recombination value. Some error will arise in the process because of the Balmer absorption lines in the underlying continuum, which tend to steepen the emission (actually, emission minus absorption) Balmer decrement while leaving most other emission lines unaffected. The galaxies discussed in this paper were chosen to have large emission line-to-continuum ratios, so that the lines could be measured well and so that errors due to underlying absorption lines would not be too large. The worst such errors may be expected to occur for A1116 + 51 and IC 3453, because these objects have relatively small Balmer-line equivalent widths and because, having no "red" spectra of these objects, we had to derive E_{B-V} from the Hγ/Hβ ratios without knowing the Hα/Hβ ratios. With possible errors of about 10% in the measured Hγ/Hβ ratios, and additional possible errors of the order of 10% due to underlying absorption lines, our estimated values of E_{B-V} might be wrong by as much as 0.2 mag for such objects. This could be the reason for the unusually high Ne^{++}/O^{++} abundance ratio obtained for A1116 + 51. On the other hand, the Hδ and Hζ intensities imply limits on the error made in E_{B-V} for this object. In the case of IC 3453, the apparent Hγ/Hβ ratio was large enough to permit us to neglect reddening; in this case, the equivalent width of any underlying Hβ absorption appears to be less than 4 Å (very likely less than 2 Å) if we are to avoid making the Hγ/Hβ ratio significantly less than observed.

Other factors can influence the reddening corrections, but these are not likely to have much effect on the critical line ratios upon which derivations of temperatures and abundances are based. Atmospheric dispersion and pointing errors should be considered. The TV guider is red-sensitive, so we generally centered the red part of the image in the aperture; and because of atmospheric dispersion, the corresponding light at shorter wavelengths may not all have passed through the aperture. This effect depends upon the distribution of light in the galaxy as well as the seeing, and increases with zenith distance. In the worst case here (A2228 − 00) a spurious E_{E-V} of roughly 0.1 mag might have been produced in this way, but generally the effect should not exceed a few hundredths of a magnitude. Pointing errors can modify this result. Differences between radial velocities measured from the emission lines, and the values given in the Second Reference Catalog (de Vaucouleurs, de Vaucouleurs, and Corwin 1976) have a mean value of − 25 km s^{-1} and an rms dispersion of ± 64 km s^{-1}. These are probably due mostly to pointing errors, and if so, indicate a rms pointing error of ± 0″.6 and a maximum pointing error of slightly more than 1″. In any single instance, an unfortunate combination of pointing errors and atmospheric dispersion might produce an error of 0.2 mag in E_{B-V}, but generally the errors will be much less. In any case, if there is some extraneous contribution to our estimated E_{B-V}, the deduced intrinsic line ratios are not correspondingly erroneous in Table 3; only the quoted values for E_{B-V} in that table would be seriously affected. In other words, our method of correcting for interstellar reddening will roughly correct for reddening produced by other causes as well.

Most of our galaxies are at high galactic latitudes where there should be little reddening by interstellar material in our own Galaxy. Hence, the substantial values of E_{B-V} found for Mrk 600 and Mrk 450 are likely to have occurred within those objects. II Zw 40, on the other hand, is at a low galactic latitude, where $E_{B-V} \approx 0.4$ is expected either from the cosecant law or from the H I column density (Jaffe, Perola, and Tarenghi 1978). The E_{B-V} reddening derived from the Balmer decrement is 0.9 mag, similar to the value given by Searle and Sargent (1972). However, Jaffe *et al.* point out that this is inconsistent with the significantly larger $E_{B-V} \approx 1.2$ deduced by them from the ratio of the 1415 MHz continuum flux to the Hβ flux in the core of this object. They propose a model with a large internal extinction ($A_V \sim 11$ mag) in addition to the foreground extinction in our Galaxy. The line *ratios*, on which our abundance and temperature estimates are based, are basically unaffected by these uncertainties. The extinction of II Zw 40 is so severe that we have only a very imperfect idea of the optical extent of the object and so the comparison of an observed optical flux (such as Hβ) with an observed radio flux (which may come from a different volume of space) is risky.

V. DISCUSSION

We find no perceptible correlation between the helium and oxygen abundances in these galaxies. Unlike Lequeux *et al.* (1979), we cannot argue that a "pregalactic" helium abundance can be found by extrapolating such a relationship to zero oxygen abundance.

We shall exclude the well-known objects I Zw 18 and II Zw 40 from the remainder of this discussion. They have been studied by a number of other authors, and there is basic agreement about their abundances. We exclude I Zw 18 because we lack a good 21 cm H I line width for it, and we exclude II Zw 40 because of the uncertainties caused by optical extinction. A discussion based on the masses of the other galaxies, which are quite uncertain, is necessarily speculative. Following Fisher and Tully (1975), we invoke the expression

$$X_{TM} = 5000(\Delta V)^2 \, aD/\sin^2 i$$

as a measure of the total mass in solar units. Here D is the distance of the galaxy in Mpc, a is its Holmberg diameter in arcmin, ΔV is the FWHM line width of the 21 cm line in km s^{-1}, and i is the inclination of the galaxy ($i = 0°$ means face-on). The inclinations of our galaxies are so uncertain
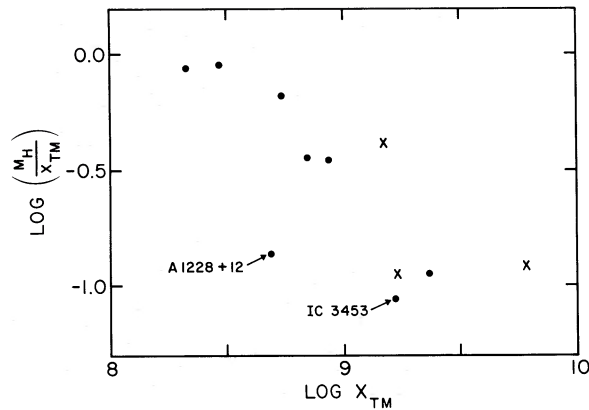
FIG. 4

FIG. 5

FIG. 4.—Plot of the log (H I mass/total mass) against the log total mass for the program galaxies (*filled circles*) and NGC 6822, LMC, and SMC (*crosses*).
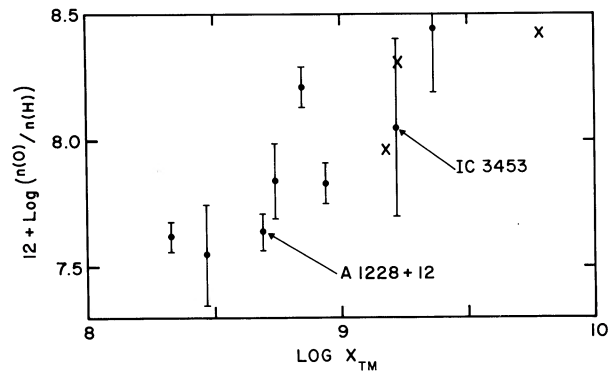
FIG. 5.—Plot of the oxygen abundance against the log total mass. Symbols are as defined for Fig. 4.

that we adopt for i a mean value of 60°. Note that a considerable error is likely to arise because ΔV, an imprecisely determined quantity, occurs as a square. Figure 4 shows a plot of the log of the ratio (H I mass)/(total mass) as a function of the log of the total mass. In addition to the galaxies listed in Table 1 (*filled circles*), we have included (as crosses) three Local Group galaxies, NGC 6822 and the Magellanic Clouds, using data from Lequeux *et al.* It is interesting to compare these Local Group galaxies with our program galaxies because their masses have been determined independently and their distances do not depend upon the Hubble constant.[3] So-called "giant" spirals have M_H/X_{TM} in the range 0.01–0.1 (Roberts 1975). Figure 4 therefore illustrates part of a general trend such that the proportion of a galaxy's mass which is H I increases as the mass of the galaxy decreases. This is often taken as evidence that star formation occurs less vigorously with decreasing galactic mass. Heavy element abundances depend upon processes that recycle material between massive stars and an interstellar medium. The abundances should depend upon the amount of past star formation and hence upon galactic mass. Figure 5, a plot of oxygen abundance $12 + \log n(O)/n(H)$ against log X_{TM}, illustrates this effect. A1228 + 12 is not anomalous in this plot, even though it was anomalous in Figure 4. We take this to mean that A1228 + 12 actually is abnormally deficient in neutral hydrogen for its total mass, and that our estimate of its total mass is not particularly bad.

Lequeux *et al.* (1979) have attempted to use the relation between abundances and (H I mass)/(total mass) ratio to distinguish between different models of galaxy evolution. Thus, if galaxies evolve as closed systems, if an instant

recycling approximation is valid, and if the initial stellar mass function and nucleosynthesis are the same for all galaxies, then the heavy element abundance Z should equal $p \ln (X_{TM}/M_H)$. Here p, known as the heavy-element yield, is defined as "the ratio of the heavy elements newly synthesized and ejected to the mass locked up in stars and stellar remnants per generation of stars." To test this, Lequeux *et al.* assume that Z is proportional to the oxygen abundance. This is a dubious assumption, since observations by Sneden, Lambert, and Whitaker (1979) of a sample of unevolved stars show a rather large scatter in the oxygen/iron ratio. Moreover, in evolved stars such as globular cluster red giants, CNO abundance anomalies relative to Fe/H are common. If we nevertheless adopt the same constant of proportionality between Z and oxygen abundance as Lequeux *et al.*, we obtain the plot of Z against $\ln (X_{TM}/M_H)$ shown in Figure 6. Here the linear relation found by Lequeux *et al.* is shown by the straight line; the agreement is adequate except for IC 3453 and A1228 + 12. Clearly our data do not have enough weight to verify the functional form predicted by this model. For instance, over the range of parameters that we have observed, there is a rough linear relation between $12 + \log n(O)/n(H)$ and $\log (M_H/X_{TM})$
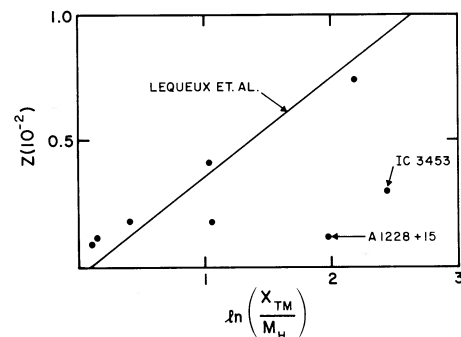
---

[3] X_{TM} and M_H depend upon D and D^2, respectively, so if we had assumed $H_0 = 100$ instead of 55 km s^{-1} Mpc^{-1}, $\log (M_H/X_{TM})$ would be smaller by 0.26. In principle, since M_H/X_{TM} should not exceed unity, we might constrain H_0 through such considerations; but in practice X_{TM} is too uncertain an approximation to the total mass for the result to be interesting.

FIG. 6.—Plot of the heavy element abundance (Z) against the natural log (total mass/H I mass) for the program galaxies.
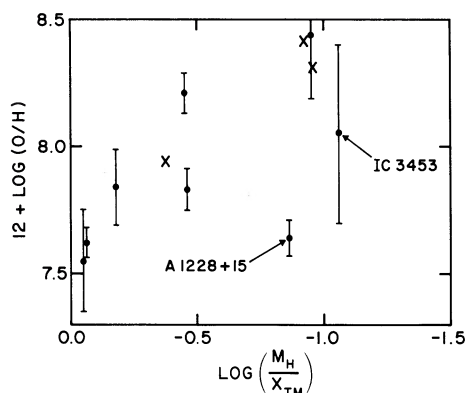
FIG. 7.—Plot of the oxygen abundance against the log (H I mass/total mass). Symbols are as defined in Fig. 4.

(Fig. 7). For reasons given above, it seems likely that A1228 + 12 and perhaps IC 3453 are abnormally deficient in H I for their mass. Both have been assumed to be members of the Virgo cluster. There is good evidence for this in the case of A1228 + 12, which has the same redshift as M87 and is located only 21' from the center of this giant elliptical galaxy. M87 has an effective radius of 15' and has been traced out to an angular radius of 30' (de Vaucouleurs 1969; Arp and Bertola 1969); we can speculate that A1228 + 12 has suffered ram-pressure ablation or some other environmental effect (cf. Gisler 1978). In this connection, we note that Chamaraux, Balkowski, and Gérard (1980) have shown that spiral galaxies in the Virgo cluster are deficient in H I by a factor of 2 when compared with galaxies of the same type which are either isolated or in small groups. They also suggest that this is produced by an environmental effect. Further observational evidence on this point is desirable.

It thus appears that in addition to uncertainties in the observations and in the derivation of physical parameters from them, differences in the environmental histories of different galaxies may prevent them from all following

any one unique model for galactic evolution. The example of A1228 + 12 is one where the environment is clearly unusual. In other cases, gas depletion might have occurred in encounters with other galaxies long enough ago that the interfering galaxies are by now well separated in space. We must also note that observational selection effects may be serious in a list of dwarf blue galaxies that have been picked out by the same technique. H II regions in a Local Group galaxy such as NGC 6822 are clearly visible, but a similar object at a distance of 10 Mpc would not be recognized as an emission-line galaxy even though it would still be discernible as a low-surface-brightness dwarf galaxy. A distant localized H II region, like a star, would decrease in brightness as the inverse square of its distance. On the other hand, an extended galaxy with nearly uniform surface brightness, measured through a small aperture of constant size, would show the same brightness regardless of distance so far as the galaxy diameter exceeds that of the measuring aperture. Thus, if a galaxy has only one or two localized active star-formation regions, and if it is observed in a particular (and common) way, the equivalent width of an emission line tends to decrease with distance. If a survey is limited by such equivalent widths, the more distant objects noted will in fact have intrinsically stronger lines compared with the entire galactic continua. This effect is quite marked in our sample of 10 galaxies. The nearer five galaxies (mean distance 14 Mpc) have an average Hβ emission equivalent width of 170 Å while the more distant five (mean distance 24 Mpc) have an average Hβ emission equivalent width of 75 Å. Finally, an interesting practical limitation on extending work of this kind is that it requires the largest radio telescopes to observe the 21 cm line in the faintest of these objects, even though optical photometry and spectroscopy are possible with rather modest optical equipment.

REFERENCES

Arp, H. C. 1965, Ap. J., 142, 402.
Arp, H. C., and Bertola, F. 1969, Ap. Letters, 4, 23.
Auer, L. H., and Mihalas, D. 1972, Ap. J. Suppl. 24, 193.
Bergeron, J. 1977, Ap. J., 211, 62.
Braccesi, A., Formiggini, L., Gioia, I., and Sargent, W. L. W. 1972, Pub. A.S.P. 84, 592.
Chamaraux, P. 1977, Astr. Ap., 60, 67.
Chamaraux, P., Balkowski, C., and Gérard, E. 1980, Astr. Ap., 83, 38.
Davidson, K. 1978, Ap. J., 220, 177.
————. 1979, Ap. J., 228, 179.
Demoulin, M.-H., and Burbidge, E. M. 1969, Ap. J. (Letters), 157, L155.
de Vaucouleurs, G. 1969, Ap. Letters, 4, 17.
de Vaucouleurs, G., de Vaucouleurs, A., and Corwin, H. G. 1976, Second Reference Catalogue of Galaxies (Austin: University of Texas Press).
Dreyer, J. L. E. 1910, Mem. R.A.S., 59, 105.
Fisher, J. R., and Tully, R. B. 1975, Astr. Ap. 44, 151.
French, H. B. 1980, Ap. J., 240, 41.
Gisler, G. R. 1978, M.N.R.A.S., 183, 633.
Gottesman, S. T., and Weliachew, L. 1972, Ap. Letters, 12, 63.
Hodge, P. W. 1971, Ann. Rev. Astr. Ap., 9, p. 35.
Huchra, J. P. 1977, Ap. J. Suppl., 35, 171.

Jaffe, W. J., Perola, G. C., and Tarenghi, M. 1978, Ap. J., 224, 808.
Kinman, T. D. 1965, Ap. J., 142, 1241.
————. 1978, in IAU Symposium 77, Structure and Properties of Nearby Galaxies, ed. E. M. Berkhuijsen and R. Wielebinski (Dordrecht: Reidel), p. 299.
Kinman, T. D. and Conklin, E. K. 1981, in preparation.
Kinman, T. D., Rubin, V. C., Thonnard, N., Ford, W. K., Jr., and Peterson, C. J. 1977, Ap. J., 82, 879.
Lequeux J., Peimbert, M., Rayo, J. F., Serrano, A. and Torres-Peimbert, S. 1979, Astr. Ap., 80, 155.
Markarian, B. E. 1969, Astrofizika, 5, 443.
————. 1972, Astrofizika, 8, 155.
————. 1973, Astrofizika, 9, 487.
Matthews, T. A., and Sandage, A. R. 1963, Ap. J., 138, 30.
Miller, J. S. 1978, Ap. J., 220, 490.
Nilsen, P. 1973, Uppsala Astr. Obs. Ann., Vol. 6 (Uppsala General Catalog of Galaxies).
————. 1974, Uppsala Astr. Obs., Reprint No. 5.
O'Connell, R. W., Thuan, T. X., and Goldstein, S. J. 1978, Ap. J. (Letters), 226, L11.
Pagel, B. E. J. 1978, M.N.R.A.S., 183, 1P.

Pagel, B. E. J., Edmunds, M. G., Fosbury, R. A. E., and Webster, B. L. 1978, *M.N.R.A.S.*, **184**, 569.

Peimbert, M., and Torres-Peimbert, S. 1974, *Ap. J.*, **193**, 327.

———. 1977, *Ap. J.*, **179**, 217.

Péquignot, D., Aldrovandi, S. M. V., and Stasinska, G. 1978, *Astr. Ap.*, **63**, 313.

Pradhan, A. K. 1974, *J. Phys. B*, **7**, L503.

———. 1976, *M.N.R.A.S.*, **177**, 31.

———. 1978, *M.N.R.A.S.*, **183**, 89P.

Reddish, V. C. 1978, *Stellar Formation* (Oxford: Pergamon), p. 227.

Roberts, M. S. 1975, in *Galaxies and the Universe*, ed. A. Sandage, M. Sandage, and J. Kristian (Chicago: University of Chicago Press), p. 309.

Rubin, V. C., Moore, S., and Bertiau, F. C. 1967, *Ap. J.*, **72**, 59.

Sandage, A. R. 1974, *Ap. J.*, **178**, 1.

Sargent, W. L. W. 1970, *Ap. J.*, **160**, 405.

Sargent, W. L. W., and Searle, L. 1970, *Ap. J. (Letters)*, **162**, L155.

Searle, L. 1976, *R.G.O. Bull.*, **182**, 119.

Searle, L., and Sargent, W. L. W. 1972, *Ap. J.*, **173**, 25.

Seaton, M. J. 1975, *M.N.R.A.S.*, **170**, 475.

Snedon, C., Lambert, D. L. and Whitaker, R. W. 1979, *Ap. J.*, **234**, 964.

van den Bergh, S. 1959, *Pub. David Dunlap. Obs.*, Vol. **2**, No. 5.

Vorontsov-Velyaminov, B. A. 1962, *Morphological Catalog of Galaxies* (Moscow: Moscow University)

Zwicky, F. 1966, *Ap. J.*, **143**, 192.

Added note.—Since completing this paper, we have seen a discussion of nearly the same topic by French (1980). The spectra of four objects—I Zw 18, II Zw 40, A1116 + 51, and A2228 − 00—were observed both by French and by us; and the two independent sets of data are in good agreement except for certain lines. He finds much less reddening than we do for A1116 + 51; presumably his result is correct, because our data for this object are very scanty. His helium-abundance estimates may be systematically lower than ours. (We think that he has underestimated the helium abundance in I Zw 18, but for the other objects we don't know whose results are better.) French's [O II]/$H\beta$ and [N II]/$H\alpha$ ratios for II Zw 40, compared with our own, suggest that these do indeed depend upon the exact region observed (see Section II above). There are some differences between his conclusions and ours, but these are too detailed to discuss here.

K. DAVIDSON: Department of Astronomy, School of Physics and Astronomy, 116 Church Street S.E., Minneapolis, MN 55455

T. D. KINMAN: Kitt Peak National Observatory, P.O. Box 26732, Tucson, AZ 85726